Inorganic Chemistry

Article

pubs.acs.org/IC

Experimental and Theoretical Study of CO_2 Insertion into Ruthenium Hydride Complexes

Srinivasan Ramakrishnan,[†,§] Kate M. Waldie,[†,§] Ingolf Warnke,[‡] Antonio G. De Crisci,[†] Victor S. Batista,*[,‡] Robert M. Waymouth,*[,†] and Christopher E. D. Chidsey*[,†]

[†]Department of Chemistry, Stanford University, Stanford, California 94305, United States

[‡]Department of Chemistry, Yale University, New Haven, Connecticut 06520-81087, United States

Supporting Information

ABSTRACT: The ruthenium hydride [RuH(CNN)(dppb)] (**1**; CNN = 2-aminomethyl-6-tolylpyridine, dppb = 1,4-bis-(diphenylphosphino)butane) reacts rapidly and irreversibly with CO_2 under ambient conditions to yield the corresponding Ru formate complex **2**. In contrast, the Ru hydride **1** reacts with acetone reversibly to generate the Ru isopropoxide, with the reaction free energy $\Delta G^{\circ}_{298\,K} = -3.1$ kcal/mol measured by ^{1}H NMR in tetrahydrofuran-d_8. Density functional theory (DFT), calibrated to the experimentally measured free energies of ketone insertion, was used to evaluate and compare the mechanism and energetics of insertion of acetone and CO_2 into the Ru−hydride bond of **1**. The calculated reaction coordinate for acetone insertion involves a stepwise outer-sphere dihydrogen transfer to acetone via hydride transfer from the metal and proton transfer from the N−H group on the CNN ligand. In contrast, the lowest energy pathway calculated for CO_2 insertion proceeds by an initial Ru−H hydride transfer to CO_2 followed by rotation of the resulting N−H-stabilized formate to a Ru−O-bound formate. DFT calculations were used to evaluate the influence of the ancillary ligands on the thermodynamics of CO_2 insertion, revealing that increasing the π acidity of the ligand cis to the hydride ligand and increasing the σ basicity of the ligand trans to it decreases the free energy of CO_2 insertion, providing a strategy for the design of metal hydride systems capable of reversible, ergoneutral interconversion of CO_2 and formate.

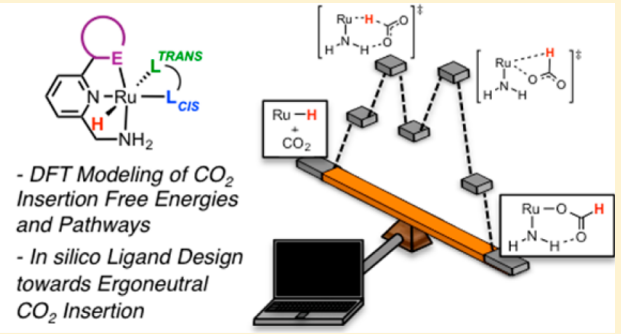

INTRODUCTION

The storage of renewable energy in chemical bonds is a promising strategy to address the intermittent nature of renewable energy sources. Carbon dioxide represents an abundant resource for this energy interconversion. The electrocatalytic hydrogenation of CO_2 to liquid fuels such as formic acid is particularly attractive because of its high energy density and convenient storage and transportation. The development of catalysts capable of selective and efficient electrocatalytic reduction of C=O bonds is essential for the implementation of such a strategy.[1−5]

The one-electron reduction of CO_2 is thermodynamically unfavorable, whereas the two-electron one-proton reduction of CO_2 to formate is greater than 1 V more positive than the one-electron reduction to $CO_2^{\bullet-}$ (−1.9 V vs NHE, pH 7).[1] Metal hydrides function as two-electron one-proton reductants, thus making hydride transfer from a transition-metal hydride complex to CO_2 an attractive route for electrocatalytic CO_2 reduction. One potential electrochemical strategy is illustrated in Scheme 1, where (a) chemical reduction of CO_2 by a metal hydride would generate a metal formate and (b) electrochemical regeneration of the metal hydride would release the formate anion.[6−10] Examples of electrocatalytic CO_2 reduction to formate using metal hydrides have been reported.[9,10]

Scheme 1. Chemical (Right) and Electrochemical (Left) Half-Cycles for Electrocatalytic CO_2 Reduction

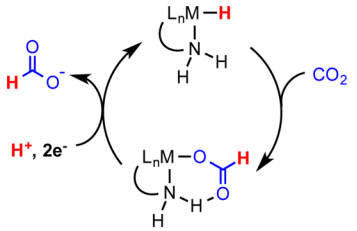

The insertion of CO_2 into a metal−hydride bond is a key step that has been the subject of much recent interest.[11−31] The energetics and rate of CO_2 insertion have been shown to vary widely with different metals and ligand environments. For efficient and reversible electrochemical CO_2 reduction, the metal hydride must be optimized such that all intermediates on the reaction coordinate for CO_2 insertion are near ergoneutral and energetic barriers are small under ambient conditions. To reach this goal, an understanding of how metal hydrides react

Received: November 5, 2015

DOI: 10.1021/acs.inorgchem.5b02556
Inorg. Chem. XXXX, XXX, XXX−XXX

Scheme 2. Proposed Transfer Hydrogenation Mechanism with Ru Hydride 1

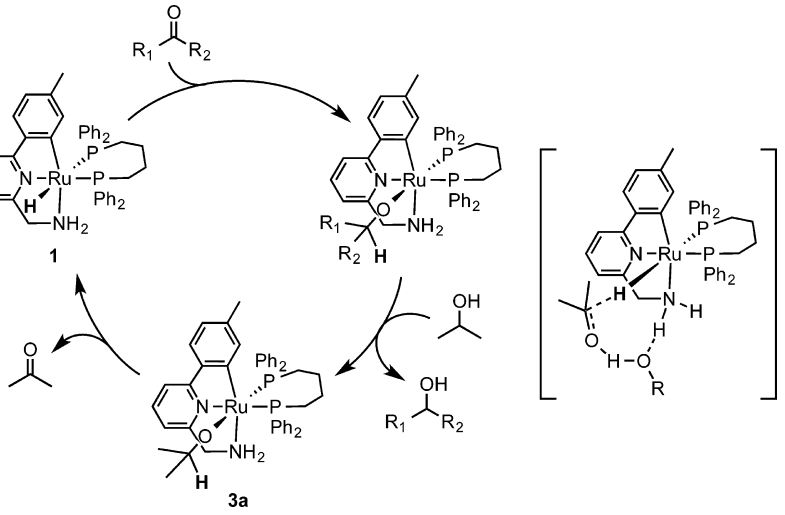

with CO_2 and what key features of the complex lead to fast and ergoneutral reactivity are needed.

We have targeted transition-metal catalysts[32,33] that rapidly catalyze ketone transfer hydrogenation[34,35] as potential candidates for ergoneutral electrocatalysis.[34,36] In a typical transfer hydrogenation scheme, the catalyst transfers a dihydrogen equivalent from a dihydrogen donor, typically isopropyl alcohol, to a ketone via a metal hydride intermediate. The ability of these catalysts to reversibly mediate this reaction under mild conditions implies that all catalytic intermediates are in rapid equilibrium and are thus at similar free energies. If such systems could be engineered to act as electrocatalysts,[36] this would ensure that ketone or CO_2 electroreduction would occur close to the thermodynamic potential.

In addition to the optimization of the thermodynamics, the kinetic barriers should also be small. A key principle derived from recent work[35,37−42] is the concept of dual-site cooperativity, whereby a metal hydride in close proximity to a Brønsted acidic site on the ligand backbone facilitates hydride and proton delivery to ketone[42−45] or CO_2.[21,30,46−49] Such bifunctional activation of C═O bonds is a promising strategy to lower kinetic barriers for CO_2 reduction.[21,30]

Baratta and co-workers reported an efficient catalyst for ketone transfer hydrogenation,[50,51] the octahedral ruthenium(II) hydride [RuH(CNN)(dppb)] (**1**) bearing an anionic tridentate CNN ligand (CNN = 2-aminomethyl-6-tolylpyridine) and a neutral bidentate phosphine (dppb = 1,4-bis(diphenylphosphino)butane). High turnover frequencies ($\sim 10^6$ h^{-1}) were reported for ketone reduction in refluxing isopropyl alcohol. Previous mechanistic and theoretical studies were consistent with a mechanism where the Ru hydride **1** reacts reversibly with ketones to generate the Ru alkoxide, which exchanges with isopropyl alcohol to liberate the product alcohol and regenerate the Ru isopropoxide **3a** (Scheme 2).[41,52,53] The primary amine on the CNN ligand was proposed to be critical to achieving efficient catalysis. Subsequent theoretical studies implicated that, in alcohol solvent, the N−H group of the ligand is part of a hydrogen-bond network that stabilizes the incipient alkoxide formed from Ru hydride addition to the ketone.[41,53]

Herein, we report experimental and theoretical studies which reveal that the Ru hydride **1** rapidly inserts CO_2 to yield the corresponding Ru formate **2** under ambient conditions. Unlike related Ru formate complexes,[21] Ru formate **2** does not readily extrude CO_2 and DFT calculations indicate that the formation of **2** from CO_2 and the Ru hydride **1** is highly exergonic. The thermodynamics and mechanism of this reaction are probed by both experiment and theory, using a DFT-based computational method validated against the experimental free energies ($\Delta G^\circ_{298\,K}$) measured for the insertion of various ketones into **1**. DFT calculations are further used to predict the influence of ancillary ligation on the energetics of CO_2 insertion to identify complexes that would enable the reversible reduction of CO_2 with ruthenium hydrides.

RESULTS AND DISCUSSION

Insertion of CO_2 into Ru Hydride 1. The Ru hydride **1** was prepared by treatment of the corresponding Ru−Cl complex with an excess of sodium isopropoxide in isopropyl alcohol/toluene at room temperature. Filtration of sodium chloride, followed by removal of the solvent from the resulting Ru isopropoxide **3a** in vacuo at room temperature, afforded the Ru hydride **1**, which was isolated as a red-orange powder. This procedure is slightly modified from that reported by Baratta,[52] as in our hands, the literature procedure afforded an inseparable mixture of chloride and hydride complexes.

The Ru hydride complex **1** reacted upon mixing with carbon dioxide to yield the Ru formate **2**[54] (Scheme 3a): when a degassed sample of **1** in tetrahydrofuran-d_8 was exposed to CO_2 at ambient pressure and temperature, the immediate and quantitative formation of the Ru formate **2** was observed by ^1H and ^{31}P NMR. The progress of this reaction could be followed by UV−visible spectroscopy in tetrahydrofuran at 298 K. Treatment of **1** (3.9×10^{-5} M) with CO_2-saturated tetrahydrofuran led to full conversion to **2** within 5 min. Analysis of the kinetics under pseudo-first-order conditions at various concentrations of [CO_2] showed the reaction to be first order in [CO_2] and first order in [**1**] according to the rate law

$$-\frac{d[\text{Ru-H } \mathbf{1}]}{dt} = k_2[\text{Ru-H } \mathbf{1}][CO_2] \quad (1)$$

where $k_2 = 29.7$ M^{-1} s^{-1}.

The Ru formate **2** is quite stable and does not readily extrude CO_2 to regenerate the Ru hydride **1**.[54] Evaporation of a tetrahydrofuran solution of **2** at 60 °C in vacuo did not lead to regeneration of **1**; attempts to induce decarboxylation at reflux

DOI: 10.1021/acs.inorgchem.5b02556
Inorg. Chem. XXXX, XXX, XXX−XXX

Scheme 3. Insertion of (a) CO_2 and (b) Ketones into the Ru−Hydride Bond of 1[a]

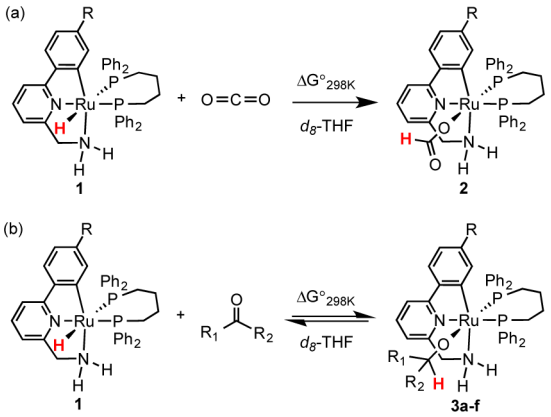

[a]R = CH_3, H for experiment and computation, respectively.

in higher-boiling solvents resulted in decomposition and formation of a black precipitate.

Thermodynamics of Carbonyl Insertion. Ketones and CO_2 both react rapidly with the Ru hydride **1**, but the thermodynamics of these two reactions differ. While ketones react reversibly with **1** and the resulting Ru alkoxides **3a−f** readily eliminate ketones to regenerate the Ru hydride **1**,[50] the equilibrium constant for the reaction of **1** with CO_2 must be considerably larger, as we were unable to regenerate **1** from the Ru formate **2** under any accessible experimental conditions. To assess the relative thermodynamics of these processes and to provide insight into the barriers and rates, experimental and theoretical studies were carried out.

To examine the thermodynamics of the reaction of **1** with ketones to form Ru alkoxides **3a−f** (Scheme 3b), the equilibrium constant for carbonyl insertion into the metal−hydride bond was determined by ^{1}H NMR. A dilute solution of the desired ketone was titrated into an 11.5 mM solution of **1** in tetrahydrofuran-d_8. Equilibration between **1** and the Ru alkoxide was rapidly established at 25 °C, and the concentrations of the different Ru complexes were determined by ^{1}H NMR. The equilibrium constants for carbonyl insertion, K_{INS}, were determined for each reaction according to eq 2, from which the insertion free energies were calculated. The results of these calculations are summarized in Table 1, entries 1−6.

$$K_{INS}(\text{ketone}) = \frac{[\text{Ru-OR } \mathbf{3a-f}]}{[\text{Ru-H } \mathbf{1}][\text{ketone}]} \quad (2)$$

For this series of ketones, the formation of the Ru alkoxides **3a−f** from the Ru hydride **1** are slightly exergonic, with $\Delta G^\circ_{298\,K}$ ranging from −1.59 to −4.22 kcal/mol. Alkoxide formation is most favorable with 4′-fluoroacetophenone, whereas formation of alkoxides from aliphatic ketones becomes less exergonic as the steric demands of the alkyl group increase, with 3,3-dimethyl-2-butanone exhibiting the least favorable insertion free energy.

These experimentally measured values for $\Delta G^\circ_{298\,K}$ of ketone insertion provide a test set of values against which DFT-based computational methods could be validated. The free energies of insertion were calculated and compared to the experimental ΔG° values. Several DFT functionals with triple-ζ basis sets on the nonmetal atoms were evaluated to reproduce the experimentally measured carbonyl insertion free energies (see

Table 1. Experimental and Computed Reaction Free Energies for Carbonyl Insertion into 1 at 298 K in Tetrahydrofuran-d_8[a]

				$\Delta G^\circ_{298\,K}$ (kcal/mol)	
entry	Ru-OR	R_1	R_2	exptl	calcd
1	**3a**	CH_3	CH_3	−3.13 ± 0.04	−2.4
2	**3b**	CH_3	n-C_5H_{11}	−2.79 ± 0.05	−2.1
3	**3c**	CH_3	$C(CH_3)_3$	−1.59 ± 0.09	−1.2
4	**3d**	CH_3	C_6H_5	−4.03 ± 0.02	−5.7
5	**3e**	CH_3	4′-F-C_6H_4	−4.22 ± 0.02	−5.9
6	**3f**	CH_3	4′-OCH_3-C_6H_4	−2.35 ± 0.03	−3.2
7	**2**		CO_2		−10.5

[a]Level of theory: ωB97xD/6-311g* (C, H, N, O, P)/LANL2DZ (Ru)/SMD (THF).

Table S4 in the Supporting Information): the best agreement was found with ωB97xD, a hybrid GGA functional with long-range dispersion corrections.[55−58] With this combination of functional and basis set, each calculated insertion free energy was within ±1.7 kcal/mol of the experimental value[59] and captured the same trends observed experimentally as the steric and electronic properties of the ketone were varied. These results indicate that this computational method is suited to capture subtle reactivity differences associated with the studied reactions.[59]

With an experimentally calibrated computational method in hand, the energetics of CO_2 insertion were evaluated computationally. The DFT-optimized structure of Ru formate **2** is in good agreement with the X-ray structure previously reported[54] (see the Supporting Information). The calculations indicate that the reaction of **1** with CO_2 is exergonic with ΔG°_{INS} = −10.5 kcal/mol (Table 1, entry 7). This corresponds to an equilibrium constant K_{INS} on the order of 5×10^7 and is consistent with our experimental observations that the Ru hydride reacts with CO_2 to generate the Ru formate, but the Ru formate does not readily eliminate CO_2 to regenerate the Ru hydride.

Calculations indicate that the dielectric constant of the solvent does not have a significant effect on the free energies for either acetone or CO_2 insertion into **1**. Employing the SMD model for other solvent dielectrics ranging from pentane (ε = 1.8) to dimethyl sulfoxide (ε = 46.8), the predicted insertion free energy values with both carbonyl substrates remain within a few kcal/mol from the tetrahydrofuran results shown in Table 1 (see the Supporting Information).

Predicted Pathway for Ketone and CO_2 Insertion. Transition-metal hydrides can react with C═O bonds by both inner-sphere and outer-sphere mechanisms.[35,38] The inner-sphere mechanism, common to many insertion reactions, requires an open coordination site for binding the C═O double bond, followed by migratory insertion of the hydride to generate an alkoxide. The outer-sphere mechanism[38,39,60] involves the cooperative transfer of the hydride from the metal and transfer of a proton from an appropriately positioned X−H bond of the ligand (typically, X = N,[38,39] O[61−63]). For a coordinatively saturated complex such as **1**, a classical inner-sphere 1,2-insertion into the Ru−hydride bond would require dissociation of an adjacent ligand.[60,64−66] Baratta and co-workers provided evidence that dissociation of the cis amine of the CNN ligand in **1** does not occur during transfer hydrogenation.[52] Similarly, we find that the rate of ketone transfer hydrogenation is not altered by the addition of excess

DOI: 10.1021/acs.inorgchem.5b02556
Inorg. Chem. XXXX, XXX, XXX−XXX

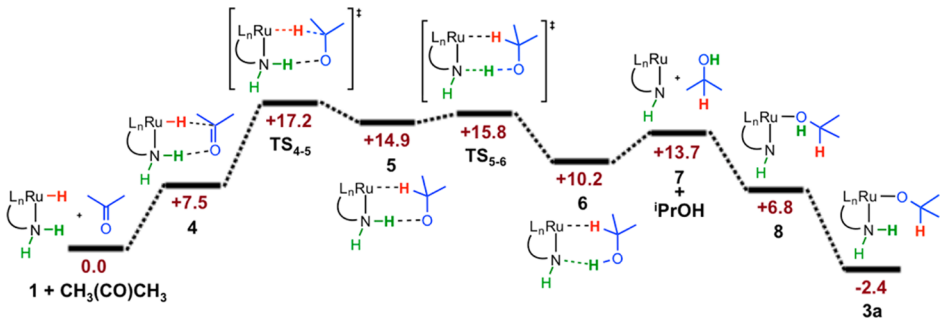

Figure 1. Calculated energy profile for the reaction of **1** with acetone. Level of theory: ωB97xD/6-311g* (C, H, N, O, P)/LANL2DZ (Ru)/SMD (THF). Free energies in kcal/mol are given relative to **1** plus acetone at 298 K. Spectator ligands are omitted for clarity.

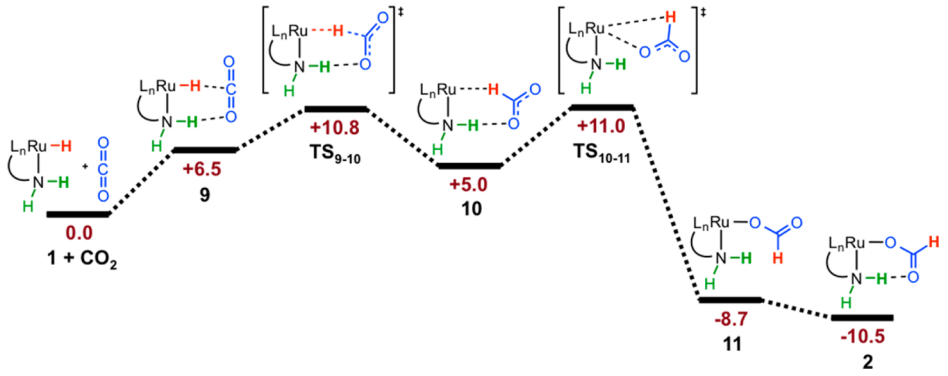

Figure 2. Calculated energy profile for the reaction of **1** with CO_2. Level of theory: ωB97xD/6-311g* (C, H, N, O, P)/LANL2DZ (Ru)/SMD (THF). Free energies in kcal/mol are given relative to **1** plus CO_2 at 298 K. Spectator ligands are omitted for clarity.

free triphenylphosphine, suggesting that dissociation of the bidentate phosphine ligand is not operative during catalysis (see the Supporting Information). From these results, we conclude that the mechanism of carbonyl insertion into **1** is unlikely to involve ancillary ligand dissociation.

Previous calculations[41] on the mechanism of transfer hydrogenation with a ruthenium hydride analogous to **1** (bearing the $Me_2P(CH_2)_4PMe_2$ (dmpb) ligand rather than $Ph_2P(CH_2)_4PPh_2$ (dppb) of **1**) in explicit alcohol solvent indicated a key role of a hydrogen-bond network (Scheme 2) to facilitate the formation of the Ru alkoxide from the Ru hydride.[41] It is important to point out that we employed a non-hydrogen-bonding solvent, tetrahydrofuran, for our studies in order to understand the reactivity purely in terms of electronic and steric contributions to the metal−ligand−substrate interactions. We utilized our calibrated DFT method to probe the energetically accessible pathways for the conversion of Ru hydride **1** and acetone into Ru isopropoxide **3a** in this solvent, as shown in Figure 1. These calculations reveal a bifunctional outer-sphere mechanism as the lowest free-energy pathway. This asynchronous delivery of dihydrogen from the Ru hydride and N−H of the coordinated amine ligand to acetone yields the Ru amide and isopropyl alcohol, which readily adds across the Ru−N bond to generate the alkoxide **3a**. Similar mechanisms have been calculated for model systems of related bifunctional Ru hydrogenation catalysts.[67,68] As indicated previously, the calculated free energy for the conversion of **1** to **3a** is, at this level of theory, within 0.7 kcal/mol of that measured experimentally.

The calculated free energy barrier for acetone insertion is $\Delta G^{\ddagger}_{298\,K}$ = 17.2 kcal/mol. This barrier would correspond to a calculated reaction rate of 1.6 s^{-1} at 25 °C, which is comparable to the initial turnover frequency of 0.5 s^{-1} measured for the transfer hydrogenation of acetophenone with isopropyl alcohol under basic conditions with catalytic amounts of the Ru chloride precatalyst at 25 °C (see the Supporting Information). These calculations reveal that a hydrogen-bonded network[41] is not necessary for the rapid and reversible interconversion of the Ru hydride **1** and the Ru isopropoxide **3a** in tetrahydrofuran. The calculated barrier for **1** is higher than that calculated for the dmpb analogue in explicit alcohol solvent,[41] but given the differences in DFT methodology and the influence of the phosphine ligands on the energetics (vide infra), it is difficult to draw any further comparisons.

Similar calculations for the reaction of Ru hydride **1** with CO_2 revealed some similarities and differences with the path calculated for acetone (Figure 2). The N−H bond of the coordinated amine of the CNN ligand plays a key role in directing the activation of CO_2 toward hydride transfer by hydrogen bonding in intermediate **9**. Hydride delivery from ruthenium to CO_2 proceeds via $\mathbf{TS_{9\text{-}10}}$ to generate **10**, a contact ion paired intermediate with a relative free energy of +5.0 kcal/mol. The energetic accessibility of $\mathbf{TS_{9\text{-}10}}$ arises from the strongly donating, anionic CNN ligand that creates an electron-rich metal and highly polarized metal−hydride bond, as well as stabilization from N−H hydrogen bonding. Outer-sphere hydride delivery without direct coordination of CO_2 to the metal center has been proposed for other metal hydride complexes,[16,69−73] as well as for the reverse process of formic acid dehydrogenation.[74] The beneficial role of hydrogen bonding with protic amine groups in the secondary coordination sphere of the metal has also been noted.[21,30]

Following the generation of the ion pair intermediate **10**, the calculations indicate that the preferred pathway leading to **2** is

DOI: 10.1021/acs.inorgchem.5b02556
Inorg. Chem. XXXX, XXX, XXX−XXX

isomerization from the N−H bound formate in **10** to a Ru-bound formate in **11** via $TS_{10\text{-}11}$, which further isomerizes to the more stable H-bonded formate **2**. The calculated barrier of 11.0 kcal/mol is in reasonable agreement with the experimentally determined barrier for CO_2 insertion, $\Delta G^{\ddagger}_{298\,K}$ = 15 kcal/mol, calculated from the rate of reaction of CO_2 with **1** using the Eyring equation (vide supra; see the Supporting Information).

Notably, the calculated barrier for the formation of the formate **2** from CO_2/**1** (11 kcal/mol) is lower than that for the formation of the alkoxide **3a** from acetone/**1** (17.2 kcal/mol). In addition, there are some key differences in the calculated reaction coordinates. The calculated pathway for acetone results in the generation of the N−H-bound isopropoxide **5** that abstracts the N−H proton to generate isopropyl alcohol and the five-coordinate Ru amide **7**. In contrast, a transition state for proton transfer from the N−H bond in **10** to formate could not be located, and all attempts to locate an on-path intermediate in which both hydrogen atoms are transferred to CO_2 converged to **10**. This is attributed to the lower basicity of the formate anion in comparison to the isopropoxide anion.

While an intermediate in which both the hydride and proton from **1** are transferred to CO_2 within the coordination sphere of the complex was not found, we calculated the energy of the analogous fully dissociated species—the five-coordinate Ru amide complex **7** and formic acid at infinite separation. As shown in Figure 3, the generation of formic acid and the amide

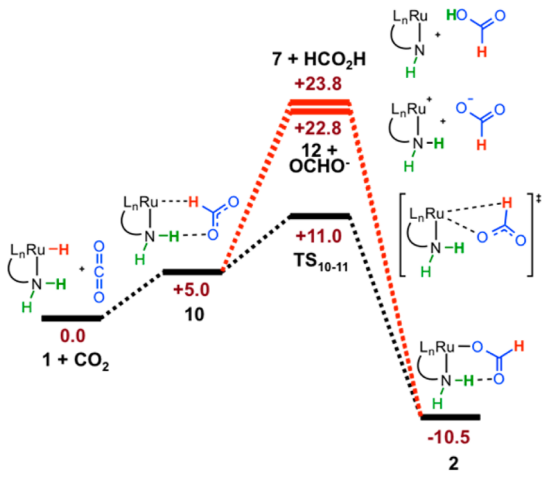

Figure 3. Energetically favorable (black) and unfavorable (red) pathways for CO_2 insertion into **1**. Level of theory: ωB97xD/6-311g* (C, H, N, O, P)/LANL2DZ (Ru)/SMD (THF). Free energies in kcal/mol are given relative to **1** plus CO_2 at 298 K. Spectator ligands are omitted for clarity.

7 is energetically unfavorable with $\Delta G^{\circ}_{298\,K}$ = +23.8 kcal/mol; therefore, we conclude that dihydrogen transfer to yield formic acid is unlikely. Dissociation of formate anion from **5** was also investigated as a possible route to Ru formate **2**; however, as seen in Figure 3, the calculated dissociation of formate from the ion pair **10** is energetically costly.

In Figure 4, the key bond distances and angles of the ion-paired formate **10** and isopropoxide **5** are compared. The formate species has a longer O−H distance between the anionic oxygen and primary amine and a larger deviation from 180° for the N−H−O angle than **28**, both of which demonstrate weaker binding of formate anion to the Ru amine in **10**. This weaker coordination enables slippage of the formate anion with a low

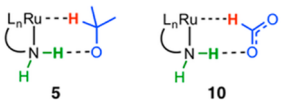

Intermediate	H---O Distance (Å)	∠NHO
5	1.54	168°
10	1.81	157°

Figure 4. Comparison of bond distances and angles for the inner-sphere ion pair intermediates **5** and **10**.

kinetic barrier. The involvement of a similar transition state for rotation of a loosely bound formate anion has been proposed for CO_2 hydrogenation catalysts.[69,70,75,76]

In Silico Approach To Engineer Ergoneutral CO_2 Insertion. The rapid and exergonic reaction of CO_2 with the Ru hydride **1** is likely a consequence of the appropriately positioned N−H bond of the coordinated amine, the presence of highly donating aryl, pyridyl, and phosphine ligands, and the strong C−H bond of the resulting formate. Nevertheless, for the design of energy-efficient electrocatalytic reactions, all intermediates should be in rapid equilibrium with small differences in free energy. While the reactivity of Ru hydride **1** with ketones is close to ergoneutral, the reaction of **1** with CO_2 is more exergonic ($\Delta G^{\circ}_{98\,K}$ = −10.5 kcal/mol). As the free energy of these reactions is likely to be sensitive to the nature of the ancillary ligation, we carried out a series of calculations to assess the influence of the ligands on the free energy of CO_2 insertion with derivatives of Ru hydride **1**.

The overall free energy for the reaction of **1** with carbonyl substrates is given by the sum of the free energies of three reactions: the hydride affinity of the substrate (acetone or CO_2), the heterolytic bond dissociation free energy of the Ru alkoxide or formate, and the hydricity of the Ru−hydride bond. This highlights the importance of considering not only the hydricity of the Ru hydride but also the heterolytic bond strength of the Ru−oxygen bond, as both are critical factors determining the overall insertion energetics for a given C═O substrate. From our calculations, the hydride affinity of CO_2 is greater than that of acetone by 23.0 kcal/mol (see section 5.7 in the Supporting Information). This inherent difference in substrate hydride affinity is counterbalanced by the difference in the heterolytic bond dissociation free energies of the Ru alkoxide and Ru formate, which results in $\Delta\Delta G^{\circ}_{INS}$ = 8.1 kcal/mol for the overall insertion free energies for acetone vs CO_2.

The steric and electronic properties of the ancillary ligands will influence the heterolytic bond free energies of the key Ru−hydride and Ru−formate bonds. Appropriate modification of the ligands will tune these bond strengths and thus tune the free energy of CO_2 insertion into the Ru−hydride bond. The effects of such modifications are modeled by our experimentally calibrated computational method in order to a priori optimize the metal hydride catalyst for ergoneutral CO_2 insertion.

To investigate the ligand influence on the thermodynamics of insertion, the ancillary ligand structure of **1** was systematically varied in silico and $\Delta G^{\circ}_{298\,K}$ for CO_2 insertion was calculated for each modified Ru hydride, as depicted in Scheme 4. The predicted free energies of CO_2 insertion into the Ru−hydride bond for these systems are presented in Table 2. We define cis and trans ligands relative to the Ru−hydride and Ru−formate bonds.

These calculations reveal that the neutral bidentate ligand in **1** has a substantial effect on the predicted thermodynamics of

DOI: 10.1021/acs.inorgchem.5b02556
Inorg. Chem. XXXX, XXX, XXX−XXX

Scheme 4. Insertion of CO_2 into the Ru−Hydride Bond of in Silico Modified Complexes

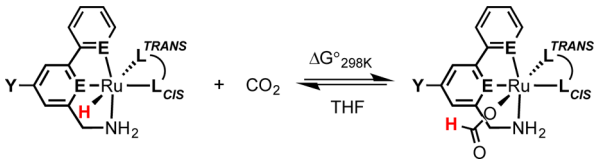

CO_2 insertion, exhibiting significant and in some cases surprising cis and trans ligand influences.[77−79] Replacement of the original π acidic phosphine ligand in **1** with the purely σ donating tetramethylenediamine ligand (Table 2, entry 2) results in an exergonic reaction with CO_2, with a calculated $\Delta G^{\circ}_{298\,K}$ = −14.5 kcal/mol. When only the cis phosphine is replaced with an amine, the reaction is even more favorable, indicating that an increase in the electron-donating capabilities of the cis ligand results in a more exergonic reaction with CO_2. The isomeric complex with an amine at the trans position (Table 2, entry 4) is also predicted to react exergonically with CO_2; however, this insertion is over 3 kcal/mol less exergonic than that for the parent Ru hydride **1**. The weaker trans influence amine in entry 4 stabilizes the Ru−hydride bond in comparison to **1** and simultaneously destabilizes the Ru−formate bond through π-donor−π-acceptor "push−pull" effects.[80] A further increase in π acidity at the cis position is explored with entry 5, for which a substantial decrease in the energetic favorability of CO_2 insertion is obtained, with $\Delta G^{\circ}_{298\,K}$ = −4.6 kcal/mol.

The trends observed for the various bidentate ligands (Table 2, entries 2−5) indicate that increasing the π acidity at the cis position results in a decrease in the $\Delta G^{\circ}_{298\,K}$ value of CO_2 insertion. Similar effects, though much smaller in magnitude, are observed when altering the π acidity of the cis pyridine ring via introduction of an electron-withdrawing trifluoromethyl or electron-donating methoxy substituent at the para position (entries 6 and 7, respectively). We also predict that switching the order of the phenyl and pyridine rings in the tridentate ligand does not have a significant effect on the energetics of CO_2 insertion (see the Supporting Information).

The series of entries 2−5 in Table 2 also demonstrates the substantial trans influence on $\Delta G^{\circ}_{298\,K}$ of insertion. We probe this behavior further by using an anionic bidentate ligand in entries 8−11. A bipyridine analogue of the tridentate ligand is selected for these systems in order to maintain an overall neutral charge on the hydride and formate complexes, as well as to simultaneously increase the π acidity in comparison to the original CNN ligand. Introduction of the strongly donating phenyl anion at the trans position results in a dramatic increase in the insertion free energy to $\Delta G^{\circ}_{298\,K}$ = −19.5 kcal/mol. CO_2

Table 2. Computed CO_2 Insertion Free Energies at 298 K in Tetrahydrofuran-d_8 for in Silico Modified Complexes

Entry	Complex	ΔG°_{298K} (kcal/mol)	Entry	Complex	ΔG°_{298K} (kcal/mol)
1	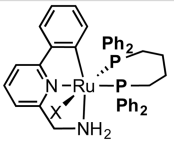	-10.5	6	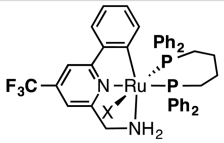	-10.0
2	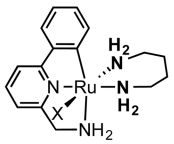	-14.5	7	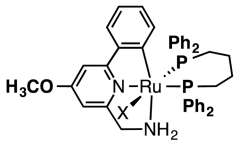	-11.0
3	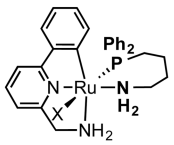	-15.3	8	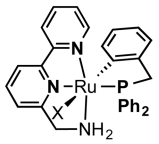	-19.5
4	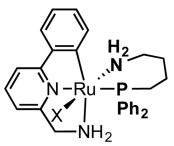	-7.4	9	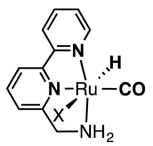	-14.5
5	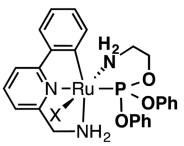	-4.6	10	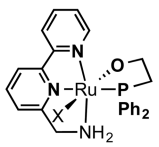	-12.2
			11	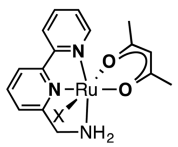	-9.8

DOI: 10.1021/acs.inorgchem.5b02556
Inorg. Chem. XXXX, XXX, XXX−XXX

insertion becomes less exergonic as the basicity of the trans anion group decreases in the order phenyl > hydride > alkoxide > acetylacetonate. Clearly, strong σ donation from an anionic ligand at the trans position is predicted to give very exergonic CO_2 insertion, which is attributed to destabilization of the Ru−hydride bond.

Overall, alteration of the electronic properties of the ancillary ligands is shown to be a powerful way to tune the free energies of CO_2 insertion into **1**. The reactivity trends from our calculations indicate that the presence of a neutral σ-donating ligand at the trans position is beneficial for decreasing the exergonicity of CO_2 insertion; however, anionic trans ligands are too strongly donating, resulting in very reactive metal hydrides that greatly favor Ru formate formation. Furthermore, we predict that the cis ligand plays a major role in determining insertion energetics, with the introduction of more π-acidic ligands at the cis position to the Ru−hydride bond being critical for attaining near-ergoneutral insertion reactivity. These predictions will guide synthetic efforts toward the preparation of optimized catalysts for CO_2 insertion.

CONCLUSIONS

Insertion of CO_2 into the Ru−hydride bond of **1** occurs rapidly under ambient conditions. While the exergonicity of this reaction precludes experimental measurement of the equilibrium constant, insertion of acetone and other ketones is near ergoneutral and the free energies for these reactions were measured by ^{1}H NMR. These results were used as a test set to select the best DFT-based method to model this class of reactions. The calibrated computational method was used to calculate the free energy of CO_2 insertion into **1** and to shed light on the mechanism for this reaction. The lowest energy predicted path for CO_2 insertion involves hydride transfer to the substrate followed by slippage of a bound formate anion to generate Ru formate **2**. Systematic tuning of the ligand environment in **1** in silico predicts that changing the electronic properties at the cis and trans positions has substantial and complementary influence on CO_2 insertion energetics. Such a calibrated computation approach will play a key role in guiding ligand design a priori for ergoneutral insertion of carbonyl substrates and predicting the energetic accessibility of relevant intermediates on the pathway for reversible CO_2 insertion.

EXPERIMENTAL SECTION

Materials and Methods. All manipulations were carried out under an inert atmosphere of nitrogen or argon with the use of standard vacuum line, Schlenk, and glovebox techniques. Solvents and ketone substrates were dried by standard methods and degassed via three freeze−pump−thaw cycles. Sodium isopropoxide (Strem Chemicals) and CO_2 (Ultra High Purity, Praxair) were used as received. 6-Bromo-2-pyridinecarboxaldehyde, 6-(4-methylphenyl)-boronic acid, and hydroxylamine hydrochloride were purchased from Sigma-Aldrich and used as received. Deuterated solvents for NMR were purchased from Cambridge Isotope Laboratories. NMR spectra were recorded on Varian 500 or 600 MHz spectrometers. Residual solvent proton and carbon peaks were used as reference. Chemical shifts are reported in parts per million (δ).

Synthesis. The CNN ligand, 2-aminomethyl-6-tolylpyridine, was synthesized by a modified procedure from the reported synthesis in order to avoid the use of cyanide reagents.[52] The Ru chloride precatalyst [RuCl(CNN)(dppb)] was prepared according to the literature procedure.[50]

6-(4-Methylphenyl)-2-pyridinecarboxaldehyde. This synthesis was based on the preparation of a similar compound.[81] 6-Bromo-2-pyridinecarboxaldehyde (5.0 g, 26.9 mmol) and $Pd(PPh_3)_4$ (0.93 g, 0.80 mmol) were dissolved in degassed toluene (50 mL) in a three-neck round-bottom flask equipped with a reflux condenser. A degassed solution of *p*-tolylboronic acid (4.0 g, 29.4 mmol) and Na_2CO_3 (5.2 g, 49.1 mmol) in methanol/water (2/3, 125 mL) was transferred to the reaction flask via cannula. The biphasic mixture was heated to reflux overnight under N_2. The mixture was diluted with dichloromethane (20 mL) and 2.0 M Na_2CO_3 (100 mL). The aqueous phase was separated and extracted with dichloromethane (3 × 50 mL). The combined organic extracts were dried over Na_2SO_4 and evaporated to a yellow residue. The crude product was purified by column chromatography on silica with 1/1 dichloromethane/hexanes, giving the product aldehyde as a white powder. Yield: 88% (4.67 g). ^{1}H NMR (300 MHz, $CDCl_3$): δ 10.16 (s, 1H), 8.00 (d, J = 8.2 Hz, 7.93−7.87 (m, 3H), 7.33 (d, J = 8.0 Hz), 2.43 (s, 3H). ^{13}C NMR (125 MHz, $CDCl_3$): δ 194.2, 158.07, 152.8, 140.0, 137.8, 135.5, 129.8, 127.0, 124.3, 119.6, 21.5.

6-(4-Methylphenyl)-2-pyridinecarboxaldehyde Oxime. A solution of 6-(4-methylphenyl)-2-pyridinecarboxyaldehyde (4.0 g, 20.3 mmol) and hydroxylamine hydrochloride (3.8 g, 54.7 mmol) in ethanol (150 mL) was stirred overnight at room temperature under N_2. The solvent was removed under reduced pressure to give a white solid, which was dissolved in dichloromethane (100 mL) and saturated Na_2HCO_3 (100 mL), and this mixture was stirred vigorously for 30 min. The aqueous layer was extracted with dichloromethane (2 × 50 mL). The combined organic extracts were dried over Na_2SO_4 and evaporated under reduced pressure to give the oxime as a white crystalline solid. Yield: 95% (4.09 g). ^{1}H NMR (300 MHz, $CDCl_3$): δ 8.95 (br s, 1H), 8.39 (s, 1H), 7.91 (d, J = 8.1 Hz, 2H), 7.75−7.69 (m, 3H), 7.29 (d, J = 8.0 Hz, 2H), 2.41 (s, 3H). ^{13}C NMR (125 MHz, $CDCl_3$) δ 157.66, 151.7, 151.6, 139.5, 137.4, 136.2, 129.7, 127.1, 120.8, 119.0, 21.5.

2-Aminomethyl-6-(4-methylphenyl)pyridine. This synthesis was based on the preparation of a similar compound reported by Baratta et al.[82] To a solution of the oxime (4.0 g, 18.8 mmol) in degassed ethanol/water (1/1, 120 mL) were added ammonium acetate (1.9 g, 24.6 mmol) and aqueous ammonia (80 mL). The solution was stirred under nitrogen for 30 min, followed by the slow addition of zinc dust (6.8 g, 104 mmol) over 2 h. The mixture was heated to reflux under N_2 for 3.5 h. After it was cooled, the mixture was filtered and the filtrate was condensed under reduced pressure. The resulting residue was basified with 1 M NaOH (100 mL) and extracted with diethyl ether (3 × 50 mL). The combined organic extracts were dried over Na_2SO_4 and evaporated to yield the crude product as a yellow oil. Purification by column chromatography on silica gave the CNN ligand as a white powder. Yield: 70% (2.62 g). NMR spectra are consistent with those reported in the literature.[52]

*[RuH(dppb)(CNN)] (**1**).* Attempts to synthesize **1** by the published procedure[52] were not successful, resulting in a mixture of chloride and hydride complexes. We prepared **1** by treatment of the Ru chloride complex [RuCl(CNN)(dppb)] with an excess of sodium isopropoxide in an isopropyl alcohol/toluene solvent mixture at room temperature. [RuCl(dppb)(CNN)] (100 mg, 0.13 mmol) was dissolved in toluene (10 mL) under argon. A solution of sodium isopropoxide (100 mg, 1.2 mmol) in isopropyl alcohol (10 mL) was prepared and added to the ruthenium chloride solution via cannula under argon. The red solution was stirred at room temperature under argon for 20 h. The solution was diluted with pentane (70 mL), cooled to −78 °C for 2 h, and then filtered through Celite. The red-orange filtrate was evaporated under reduced pressure. The resulting orange residue was washed with isopropyl alcohol (10 × 1 mL) and dried under vacuum to give **1**. Yield: 56% (53 mg). NMR spectra are consistent with literature values.[50]

*[Ru(OCHO)(dppb)(CNN)] (**2**).* Ru hydride **1** (5.0 mg, 0.0069 mmol) was dissolved in tetrahydrofuran-d_8 (0.6 mL) in a sealable NMR tube in an inert-atmosphere glovebox. The sample was degassed by three freeze−pump−thaw cycles and then refilled with carbon dioxide. The solution changed from orange to yellow upon mixing, consistent with insertion of CO_2 to yield the Ru formate **2**. Full conversion of Ru hydride **1** was confirmed by ^{1}H and ^{31}P NMR. Spectra are consistent with those reported in the literature.[54]

DOI: 10.1021/acs.inorgchem.5b02556
Inorg. Chem. XXXX, XXX, XXX−XXX

Representative Procedure for NMR Equilibrium Studies with 1. In a typical experiment, **1** (5.0 mg, 0.0069 mmol) was dissolved in tetrahydrofuran-d_8 (0.6 mL) with the internal standard *p*-xylene (0.0081 mmol) in a sealable NMR tube in an inert-atmosphere glovebox. A solution of ketone (0.10−0.19 M) was prepared in tetrahydrofuran-d_8, which was added in 25 μL aliquots via gastight syringe under inert conditions. After each aliquot addition, the solution was equilibrated at 25 °C prior to recording the ^{1}H NMR spectrum. Conversion of **1** and formation of Ru alkoxide were determined from their integrations relative to the internal standard.

Computational Details. All Kohn−Sham density functional[83−85] calculations were performed using the long-range corrected hybrid functional ωB97xD.[55−58] Basis sets of triple-ζ quality plus polarization functions (6-311G*)[86−89] were used for all non-hydrogen atoms except ruthenium. Polarization functions were omitted for hydrogen atoms nonessential to the reaction pathway. Hydrogen atoms on the primary amine of the CNN ligand as well as those transferred between the alcohol and the complex were described by the same triple-ζ basis set along with added polarization and diffuse functions. The LANL2DZ basis set[90,91] of double-ζ quality was employed for ruthenium. The corresponding Los Alamos effective core potentials included one-electron velocity and Darwin relativistic effects. All calculations were performed using the quantum chemistry software package Gaussian09.[92] Geometry optimizations were performed in the gas phase using tight convergence criteria and ultrafine integration grids for the four-center−two-electron integrals. We used this method to overcome convergence issues in the self-consistent-field iterations. Gaussian09's QST2 and QST3 algorithms were used to locate transition states, which were subsequently verified by structure reoptimization after subjection to small perturbations along their imaginary mode (performed twice in opposite directions to recover reactants and products). In addition, intrinsic reaction coordinate (IRC)[93] analyses were performed for all transition states in the forward and reverse directions and the end points of the obtained paths were optimized to locate stationary points connected by the respective transition states.

The SMD[94] polarizable continuum solvation model was employed to account for nonspecific solute−solvent interactions. To compute gas-phase reaction free energies, reactants and products were optimized in vacuo to obtain geometries and electronic energies. Using the gas phase optimized structures, harmonic frequency calculations were performed to obtain thermal corrections to the Gibbs free energies.[95,96] The free energies of solvation of the reaction partners $\Delta_{sol}G(\text{reac})$ and $\Delta_{sol}G(\text{prod})$ were computed for the gas-phase minimum energy configurations. The reaction free energy change in solution is thus approximated by eq 3:

$$\Delta_r G(s) = \Delta_r G(g) + \Delta_{sol}G(\text{prod}) - \Delta_{sol}G(\text{reac}) \quad (3)$$

Standard-state corrections were applied to account for free energy change in an ideal gas when the concentration was increased from 1 mol per 24.46 L to 1 mol per 1 L, as shown in eq 4:

$$\Delta_{sol}G^{\circ\longrightarrow *} = RT \ln\ 24.46 = 1.89 \text{ kcal/mol} \quad (4)$$

■ ASSOCIATED CONTENT

Supporting Information

The Supporting Information is available free of charge on the ACS Publications website at DOI: 10.1021/acs.inorgchem.5b02556.

NMR spectra, UV/vis absorbance data and CO_2 insertion kinetics, ketone insertion equilibria, transfer hydrogenation experimental details, DFT energies and coordinates of intermediates and transition states, sample input files, comparison of X-ray and DFT structures of **2**, tabulated insertion energies computed for a range of solvents, example thermochemical cycle, and bond length changes during key transition states (PDF)

■ AUTHOR INFORMATION

Corresponding Authors

*E-mail for V.S.B.: victor.batista@yale.edu.
*E-mail for R.M.W.: waymouth@stanford.edu.
*E-mail for C.E.D.C.: chidsey@stanford.edu.

Author Contributions

§These authors contributed equally to this work.

Notes

The authors declare no competing financial interest.

■ ACKNOWLEDGMENTS

This material is based on work supported by the Global Climate and Energy Program at Stanford, the National Science Foundation (NSF-CHE 1213403), and as part of the Center for Electrocatalysis, Transport Phenomena, and Materials (CETM) for Innovative Energy Storage, an Energy Frontier Research Center funded by the U.S. Department of Energy, Office of Science, Office of Basic Energy Sciences, under Award Number DE-SC00001055. S.R., K.M.W., and A.G.D.C. are grateful for Center for Molecular Analysis and Design (CMAD) fellowships; K.M.W. is grateful for a Gabilan Stanford Graduate Fellowship and a National Science and Engineering Research Council of Canada Postgraduate Scholarship. We thank Dr. J. B. Gary for useful discussions.

■ REFERENCES

(1) Appel, A. M.; Bercaw, J. E.; Bocarsly, A. B.; Dobbek, H.; DuBois, D. L.; Dupuis, M.; Ferry, J. G.; Fujita, E.; Hille, R.; Kenis, P. J. A.; Kerfeld, C. A.; Morris, R. H.; Peden, C. H. F.; Portis, A. R.; Ragsdale, S. W.; Rauchfuss, T. B.; Reek, J. N. H.; Seefeldt, L. C.; Thauer, R. K.; Waldrop, G. L. *Chem. Rev.* **2013**, *113*, 6621.
(2) Rakowski DuBois, M.; DuBois, D. L. *Acc. Chem. Res.* **2009**, *42*, 1974.
(3) Benson, E. E.; Kubiak, C. P.; Sathrum, A. J.; Smieja, J. M. *Chem. Soc. Rev.* **2009**, *38*, 89.
(4) Joó, F. *ChemSusChem* **2008**, *1*, 805.
(5) Costentin, C.; Robert, M.; Savéant, J.-M. *Chem. Soc. Rev.* **2013**, *42*, 2423.
(6) Bolinger, C. M.; Story, N.; Sullivan, B. P.; Meyer, T. J. *Inorg. Chem.* **1988**, *27*, 4582.
(7) Caix, C.; Chardon-Noblat, S.; Deronzier, A.; Ziessel, R. *J. Electroanal. Chem.* **1993**, *362*, 301.
(8) Caix, C.; Chardon-Noblat, S.; Deronzier, A. *J. Electroanal. Chem.* **1997**, *434*, 163.
(9) Pugh, J. R.; Bruce, M. R. M.; Sullivan, B. P.; Meyer, T. J. *Inorg. Chem.* **1991**, *30*, 86.
(10) Kang, P.; Cheng, C.; Chen, Z.; Schauer, C. K.; Meyer, T. J.; Brookhart, M. *J. Am. Chem. Soc.* **2012**, *134*, 5500.
(11) Darensbourg, D. J.; Rokicki, A.; Darensbourg, M. Y. *J. Am. Chem. Soc.* **1981**, *103*, 3223.
(12) Sullivan, B. P.; Meyer, T. J. *Organometallics* **1986**, *5*, 1500.
(13) Darensbourg, D. J.; Wiegreffe, P.; Riordan, C. G. *J. Am. Chem. Soc.* **1990**, *112*, 5759.
(14) Darensbourg, D. J.; Wiegreffe, H. P.; Wiegreffe, P. W. *J. Am. Chem. Soc.* **1990**, *112*, 9252.
(15) Whittlesey, M. K.; Perutz, R. N.; Moore, M. H. *Organometallics* **1996**, *15*, 5166.
(16) Konno, H.; Kobayashi, A.; Sakamoto, K.; Fagalde, F.; Katz, N. E.; Saitoh, H.; Ishitani, O. *Inorg. Chim. Acta* **2000**, *299*, 155.
(17) Field, L. D.; Lawrenz, E. T.; Shaw, W. J.; Turner, P. *Inorg. Chem.* **2000**, *39*, 5632.
(18) DuBois, D. L.; Berning, D. E. *Appl. Organomet. Chem.* **2000**, *14*, 860.
(19) Hayashi, H.; Ogo, S.; Abura, T.; Fukuzumi, S. *J. Am. Chem. Soc.* **2003**, *125*, 14266.

DOI: 10.1021/acs.inorgchem.5b02556
Inorg. Chem. XXXX, XXX, XXX−XXX

(20) Jessop, P. G.; Joó, F.; Tai, C.-C. *Coord. Chem. Rev.* **2004**, *248*, 2425.
(21) Koike, T.; Ikariya, T. *Adv. Synth. Catal.* **2004**, *346*, 37.
(22) Creutz, C.; Chou, M. H. *J. Am. Chem. Soc.* **2007**, *129*, 10108.
(23) Tanaka, R.; Yamashita, M.; Nozaki, K. *J. Am. Chem. Soc.* **2009**, *131*, 14168.
(24) Creutz, C.; Chou, M. H.; Hou, H.; Muckerman, J. T. *Inorg. Chem.* **2010**, *49*, 9809.
(25) Federsel, C.; Boddien, A.; Jackstell, R.; Jennerjahn, R.; Dyson, P. J.; Scopelliti, R.; Laurenczy, G.; Beller, M. *Angew. Chem., Int. Ed.* **2010**, *49*, 9777.
(26) Chakraborty, S.; Zhang, J.; Krause, J. A.; Guan, H. *J. Am. Chem. Soc.* **2010**, *132*, 8872.
(27) Rankin, M. A.; Cummins, C. C. *J. Am. Chem. Soc.* **2010**, *132*, 10021.
(28) Langer, R.; Diskin-Posner, Y.; Leitus, G.; Shimon, L. J. W.; Ben-David, Y.; Milstein, D. *Angew. Chem., Int. Ed.* **2011**, *50*, 9948.
(29) Tanaka, R.; Yamashita, M.; Chung, L. W.; Morokuma, K.; Nozaki, K. *Organometallics* **2011**, *30*, 6742.
(30) Schmeier, T. J.; Dobereiner, G. E.; Crabtree, R. H.; Hazari, N. *J. Am. Chem. Soc.* **2011**, *133*, 9274.
(31) Matsubara, Y.; Fujita, E.; Doherty, M. D.; Muckerman, J. T.; Creutz, C. *J. Am. Chem. Soc.* **2012**, *134*, 15743.
(32) Perry, R. H.; Brownell, K. R.; Chingin, K.; Cahill, T. J.; Waymouth, R. M.; Zare, R. N. *Proc. Natl. Acad. Sci. U. S. A.* **2012**, *109*, 2246.
(33) Brownell, K. R.; McCrory, C. C. L.; Chidsey, C. E. D.; Perry, R. H.; Zare, R. N.; Waymouth, R. M. *J. Am. Chem. Soc.* **2013**, *135*, 14299.
(34) Trincado, M.; Banerjee, D.; Gruetzmacher, H. *Energy Environ. Sci.* **2014**, *7*, 2464.
(35) Wang, D.; Astruc, D. *Chem. Rev.* **2015**, *115*, 6621.
(36) Bonitatibus, P. J.; Rainka, M. P.; Peters, A. J.; Simone, D. L.; Doherty, M. D. *Chem. Commun.* **2013**, *49*, 10581.
(37) Haack, K.-J.; Hashiguchi, S.; Fujii, A.; Ikariya, T.; Noyori, R. *Angew. Chem., Int. Ed. Engl.* **1997**, *36*, 285.
(38) Yamakawa, M.; Ito, H.; Noyori, R. *J. Am. Chem. Soc.* **2000**, *122*, 1466.
(39) Noyori, R.; Yamakawa, M.; Hashiguchi, S. *J. Org. Chem.* **2001**, *66*, 7931.
(40) Casey, C. P.; Johnson, J. B. *J. Org. Chem.* **2003**, *68*, 1998.
(41) Baratta, W.; Baldino, S.; Calhorda, M. J.; Costa, P. J.; Esposito, G.; Herdtweck, E.; Magnolia, S.; Mealli, C.; Messaoudi, A.; Mason, S. A.; Veiros, L. F. *Chem. - Eur. J.* **2014**, *20*, 13603.
(42) Dub, P. A.; Ikariya, T. *J. Am. Chem. Soc.* **2013**, *135*, 2604.
(43) Prokopchuk, D. E.; Morris, R. H. *Organometallics* **2012**, *31*, 7375.
(44) Dub, P. A.; Henson, N. J.; Martin, R. L.; Gordon, J. C. *J. Am. Chem. Soc.* **2014**, *136*, 3505.
(45) Morris, R. H. *Acc. Chem. Res.* **2015**, *48*, 1494.
(46) Badiei, Y. M.; Wang, W.-H.; Hull, J. F.; Szalda, D. J.; Muckerman, J. T.; Himeda, Y.; Fujita, E. *Inorg. Chem.* **2013**, *52*, 12576.
(47) Bays, J. T.; Priyadarshani, N.; Jeletic, M. S.; Hulley, E. B.; Miller, D. L.; Linehan, J. C.; Shaw, W. J. *ACS Catal.* **2014**, *4*, 3663.
(48) Onishi, N.; Xu, S.; Manaka, Y.; Suna, Y.; Wang, W.-H.; Muckerman, J. T.; Fujita, E.; Himeda, Y. *Inorg. Chem.* **2015**, *54*, 5114.
(49) Lilio, A. M.; Reineke, M. H.; Moore, C. E.; Rheingold, A. L.; Takase, M. K.; Kubiak, C. P. *J. Am. Chem. Soc.* **2015**, *137*, 8251.
(50) Baratta, W.; Chelucci, G.; Gladiali, S.; Siega, K.; Toniutti, M.; Zanette, M.; Zangrando, E.; Rigo, P. *Angew. Chem., Int. Ed.* **2005**, *44*, 6214.
(51) Chelucci, G.; Baldino, S.; Baratta, W. *Coord. Chem. Rev.* **2015**, *300*, 29.
(52) Baratta, W.; Bosco, M.; Chelucci, G.; Del Zotto, A.; Siega, K.; Toniutti, M.; Zangrando, E.; Rigo, P. *Organometallics* **2006**, *25*, 4611.
(53) Baratta, W.; Ballico, M.; Esposito, G.; Rigo, P. *Chem. - Eur. J.* **2008**, *14*, 5588.
(54) Baratta, W.; Ballico, M.; Del Zotto, A.; Herdtweck, E.; Magnolia, S.; Peloso, R.; Siega, K.; Toniutti, M.; Zangrando, E.; Rigo, P. *Organometallics* **2009**, *28*, 4421.
(55) Becke, A. D. *J. Chem. Phys.* **1997**, *107*, 8554.
(56) Grimme, S. *J. Comput. Chem.* **2006**, *27*, 1787.
(57) Chai, J.-D.; Head-Gordon, M. *Phys. Chem. Chem. Phys.* **2008**, *10*, 6615.
(58) Minenkov, Y.; Singstad, A.; Occhipinti, G.; Jensen, V. R. *Dalton Trans.* **2012**, *41*, 5526.
(59) Cramer, C. J.; Truhlar, D. G. *Phys. Chem. Chem. Phys.* **2009**, *11*, 10757.
(60) Samec, J. S. M.; Bäckvall, J.-E.; Andersson, P. G.; Brandt, P. *Chem. Soc. Rev.* **2006**, *35*, 237.
(61) Shvo, Y.; Czarkie, D.; Rahamim, Y.; Chodosh, D. F. *J. Am. Chem. Soc.* **1986**, *108*, 7400.
(62) Conley, B. L.; Pennington-Boggio, M. K.; Boz, E.; Williams, T. J. *Chem. Rev.* **2010**, *110*, 2294.
(63) Casey, C. P.; Guan, H. R. *J. Am. Chem. Soc.* **2009**, *131*, 2499.
(64) Bryndza, H. E.; Calabrese, J. C.; Marsi, M.; Roe, D. C.; Tam, W.; Bercaw, J. E. *J. Am. Chem. Soc.* **1986**, *108*, 4805.
(65) Itagaki, H.; Koga, N.; Morokuma, K.; Saito, Y. *Organometallics* **1993**, *12*, 1648.
(66) Martín-Matute, B.; Aberg, J. B.; Edin, M.; Bäckvall, J.-E. *Chem. - Eur. J.* **2007**, *13*, 6063.
(67) Hadzovic, A.; Song, D.; MacLaughlin, C. M.; Morris, R. H. *Organometallics* **2007**, *26*, 5987.
(68) Hasanayn, F.; Morris, R. H. *Inorg. Chem.* **2012**, *51*, 10808.
(69) Li, J.; Yoshizawa, K. *Bull. Chem. Soc. Jpn.* **2011**, *84*, 1039.
(70) Kumar, N.; Camaioni, D. M.; Dupuis, M.; Raugei, S.; Appel, A. M. *Dalton Trans.* **2014**, *43*, 11803.
(71) Gao, H.; Chen, L.; Chen, J.; Guo, Y.; Ye, D. *Catal. Sci. Technol.* **2015**, *5*, 1006.
(72) Ohnishi, Y.-y.; Nakao, Y.; Sato, H.; Sakaki, S. *Organometallics* **2006**, *25*, 3352.
(73) Filonenko, G. A.; Smykowski, D.; Szyja, B. M.; Li, G.; Szczygieł, J.; Hensen, E. J. M.; Pidko, E. A. *ACS Catal.* **2015**, *5*, 1145.
(74) Yang, X. *Dalton Trans.* **2013**, *42*, 11987.
(75) Urakawa, A.; Jutz, F.; Laurenczy, G.; Baiker, A. *Chem. - Eur. J.* **2007**, *13*, 3886.
(76) Urakawa, A.; Iannuzzi, M.; Hutter, J.; Baiker, A. *Chem. - Eur. J.* **2007**, *13*, 6828.
(77) Coe, B. J.; Glenwright, S. J. *Coord. Chem. Rev.* **2000**, *203*, 5.
(78) Greif, A. H.; Hrobárik, P.; Hrobáriková, V.; Arbuznikov, A. V.; Autschbach, J.; Kaupp, M. *Inorg. Chem.* **2015**, *54*, 7199.
(79) Chatt, J.; Shaw, B. L. *J. Chem. Soc.* **1962**, 5075.
(80) Poulton, J. T.; Folting, K.; Streib, W. E.; Caulton, K. G. *Inorg. Chem.* **1992**, *31*, 3190.
(81) Jensen, M. P.; Lange, S. J.; Mehn, M. P.; Que, E. L.; Que, L., Jr *J. Am. Chem. Soc.* **2003**, *125*, 2113.
(82) Baratta, W.; Chelucci, G.; Magnolia, S.; Siega, K.; Rigo, P. *Chem. - Eur. J.* **2009**, *15*, 726.
(83) Parr, R. G.; Yang, W. *Density Functional Theory of Atoms and Molecules*; Oxford University Press: New York, 1989.
(84) Hohenberg, P.; Kohn, W. *Phys. Rev.* **1964**, *136*, B864.
(85) Kohn, W.; Sham, L. J. *Phys. Rev.* **1965**, *140*, A1133.
(86) Clark, T.; Chandrasekhar, J.; Spitznagel, G. W.; Schleyer, P. V. R. *J. Comput. Chem.* **1983**, *4*, 294.
(87) Frisch, M. J.; Pople, J. A.; Binkley, J. S. *J. Chem. Phys.* **1984**, *80*, 3265.
(88) Krishnan, R.; Binkley, J. S.; Seeger, R.; Pople, J. A. *J. Chem. Phys.* **1980**, *72*, 650.
(89) Mitin, A. V.; Baker, J.; Pulay, P. *J. Chem. Phys.* **2003**, *118*, 7775.
(90) Wadt, W. R.; Hay, P. J. *J. Chem. Phys.* **1985**, *82*, 284.
(91) Hay, P. J.; Wadt, W. R. *J. Chem. Phys.* **1985**, *82*, 270.
(92) Frisch, M. J., et al. *Gaussian 09, revision C.01*; Gaussian, Inc., Wallingford, CT, 2010.
(93) Fukui, K. *Acc. Chem. Res.* **1981**, *14*, 363.
(94) Marenich, A. V.; Cramer, C. J.; Truhlar, D. G. *J. Phys. Chem. B* **2009**, *113*, 6378.
(95) Ribeiro, R. F.; Marenich, A. V.; Cramer, C. J.; Truhlar, D. G. *J. Phys. Chem. B* **2011**, *115*, 14556.

DOI: 10.1021/acs.inorgchem.5b02556
Inorg. Chem. XXXX, XXX, XXX−XXX

(96) Ho, J.; Klamt, A.; Coote, M. L. *J. Phys. Chem. A* **2010**, *114*, 13442.

DOI: 10.1021/acs.inorgchem.5b02556
Inorg. Chem. XXXX, XXX, XXX−XXX